Time-resolved structural study of low-index surfaces of germanium near its bulk melting temperature

Xinglin Zeng and H. E. Elsayed-Ali*
Department of Electrical and Computer Engineering, Old Dominion University, Norfolk, Virginia 23529
(Received 24 October 2000; revised manuscript received 16 April 2001; published 7 August 2001)

The structure of the low-index surfaces of germanium near its bulk melting temperature is investigated using 100-ps time-resolved reflection high-energy electron diffraction. The surface is heated by 100-ps laser pulses while a synchronized electron beam probes the structure. Ge(111) was observed to remain in its incomplete melting structure up to at least $T_m+134\pm40$ K when heated by a 100-ps laser pulse. Both the Ge(100) and Ge(110) surfaces are observed to melt near the bulk melting temperature when heated with 100-ps laser pulses. Because of the low-diffraction intensity-to-background ratio at high temperatures and because of the temperature uncertainty in the time-resolved experiments, we are unable to accurately identify the melting point of Ge(100) and Ge(110) when heated with a 100-ps laser pulse. The results, however, favor the lack of surface superheating of Ge(100) and, to some extent, Ge(110). The superheating of the incomplete melting state of Ge(111) could be due to the metallization of the top germanium bilayer and its interaction with the solid underneath causing an energy barrier sufficient to allow for transient surface superheating.

DOI: 10.1103/PhysRevB.64.085410 PACS number(s): 68.35.−p, 68.08.−p, 61.14.−x

I. INTRODUCTION

While the melting of solids has been studied for many decades, our understanding of melting is mainly on the thermodynamical level, which does not describe the atomic process during melting. Melting is believed to start from surfaces and extended defects. Surface disorder has been investigated using molecular-dynamics (MD) simulations in which the surface structure is modeled by an appropriate potential. Several fcc metals have been studied using MD simulations including Al,[1–4] Au,[5–11] Cu,[12–17] Ni,[18–19] and Pb.[20] The general observation of MD simulations suggests that the propensity of a surface to remain ordered up to the bulk melting point (T_m) is influenced by the surface orientation, in agreement with the experimental studies. Close-packed surfaces such as fcc(111) have been observed to remain ordered up to T_m, while the open surfaces such as fcc(110) premelt below the bulk melting temperature.

Supercooling of the melt has been observed for many years, while the superheating of the solid is rarely observed due to premelting (disorder) of the surface below the bulk melting point.[21] Close-packed surfaces that do not premelt have been observed to superheat under certain conditions. Superheating of Pb(111) and Bi(0001) was observed in time-resolved reflection high-energy electron diffraction (RHEED).[22–26] Di Tolla, Ercolessi, and Tosatti have developed a thermodynamic model on the superheating of crystals.[27] In their model, a melting surface is obtained when $\Delta\gamma_\infty<0$, where $\Delta\gamma_\infty=\gamma_{SL}+\gamma_{LV}-\gamma_{SV}$ is the net free-energy change upon conversion of the solid-vapor (SV) interface in two noninteracting solid-liquid (SL), and liquid-vapor (LV) interfaces separated by an infinite liquid thickness. For a melting surface, the surface starts to melt at a wetting temperature T_w below the bulk melting point T_m. The wetting temperature is given by $T_w=T_m(1-|\Delta\gamma_\infty|/L\rho\xi)$, where ξ is the correlation length between the SL and LV interfaces mediated by the liquid, ρ is the liquid density, and L is the latent heat of melting. The thickness of the liquid layer is given by $d(T)=\xi\ln[T_m|\Delta\gamma_\infty|/(T_m-T)L\rho\xi]$.[27] The thickness of the liquid layer grows logarithmically with increasing temperature and divergences at $T=T_m$, which is in agreement with the experimental observation.[28–31] Surface melting below the bulk melting temperature was observed on some open fcc metals such as Pb(110) and Al(110).[28–31] A nonmelting surface is obtained when $\Delta\gamma_\infty>0$. In this case, melting below T_m is energetically unfavorable, and an energy barrier for melting exists up to a temperature $T_s=T_m(1+\Delta\gamma_\infty/L\rho\xi)$, which is above the bulk melting temperature. Above T_s the surface melts. The metastable state at $T_m<T<T_s$ is called the superheated (overheated) state.[27] T_s is the maximum superheating temperature. Therefore, a surface with nonmelting behavior could be superheated.

For Germanium, $\Delta\gamma_\infty=43\,\mathrm{mJ\,cm^{-2}}$.[32] This value is for an average atomic surface packing density and does not consider the effect of the surface orientation. $\Delta\gamma_\infty$ is, however, dependent on the surface orientation; $\Delta\gamma_\infty$ is higher for the close-packed surfaces like fcc(111) and fcc(100) than for open surfaces such as fcc(110).[33] The studies on Pb low-index surfaces provide an experimental evident on the dependence of the surface melting behavior on the surface orientation. Our time-resolved RHEED provides a way to transiently heat the surface to a state above the bulk melting temperature in a 100-ps time scale, while the synchronized 100-ps electron pulse probes the surface structure. A similar pump-probe technique, time-resolved low-energy electron diffraction (LEED), was first used by Becker, Golovchenko and Swartzentruber to investigate pulsed laser annealing of the Ge(111) surface with nanosecond temporal resolution.[34] While the orientation dependence of the structural properties of 100-ps laser-heated metal surfaces was studied before,[26] no such a study was conducted before on a semiconductor surface. Germanium offers an excellent semiconductor material to study this orientation dependence of the transient structural properties at high temperatures because it is an

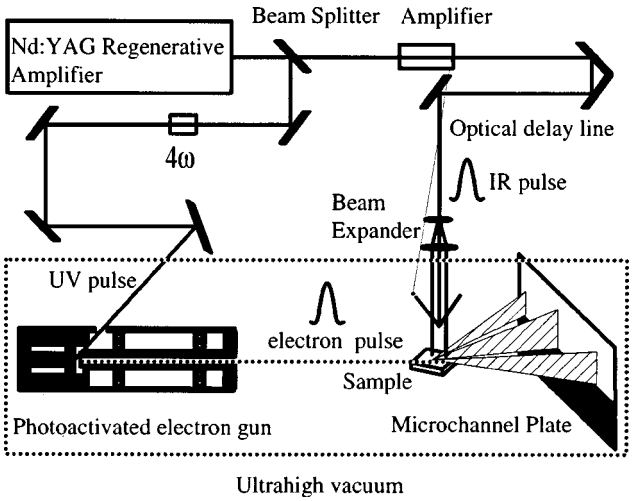

FIG. 1. Experimental setup for time-resolved reflection high-energy electron diffraction. The fundamental of a Nd:YAG laser ($\lambda = 1.06\ \mu$m, FWHM$=100$ ps) is split into two beams. The first is amplified and heats the sample surface. The second is frequency quadrupled to the ultraviolet ($\lambda = 0.266\ \mu$m) and is incident on the cathode of a photoactivated electron gun producing electron pulses synchronized with the laser pulses and used for RHEED.

elemental semiconductor with low vapor pressure near T_m, which allows conducting experiments without interference of significant surface evaporation effects. This is not the case for Si because it has a significant vapor pressure near its bulk T_m. In this paper, we present time-resolved RHEED experiments on the three low-index surfaces of Ge in order to investigate the melting behavior of these surfaces under ultrafast laser transient heating. Following a brief description of the experimental method in Sec. II, we present in Sec. III results of the structural studies of Ge(111), Ge(100), and Ge(110) at high temperatures near the bulk melting point. The results are summarized in Sec. IV.

II. EXPERIMENTAL METHODS

The experiments are performed on the time-resolved reflection high-energy electron diffraction system schematically shown in Fig. 1.[35–36] The fundamental beam of a Nd:YAG laser ($\lambda = 1.06\ \mu$m, full width at half maximum (FWHM) $= 100$ ps) is split into two beams. The first beam is amplified and interacts with the sample surface at near-normal incidence, providing a pulsed transient heating source. The second beam is frequency quadrupled to the ultraviolet ($\lambda = 0.266\ \mu$m) and is incident on the cathode of a photoactivated electron gun, producing electron pulses. The strong acceleration electric field ($\sim$6 kV/mm) between the cathode and the extraction pinhole minimizes space-charge effects that, otherwise, could cause the temporal broadening of the electron pulse. Therefore, The temporal width of the electron pulse is comparable to that of the fundamental laser pulse. The resulting electron pulses, with 50-Hz repetition rate, at which the laser operates, are incident on the surface of the sample in the glancing angle of the RHEED geometry, and hence, probe the first few atomic layers. The diffracted electrons are amplified by a chevron microchannel plate assembly proximity focused to a phosphor screen. The resulting RHEED pattern on the phosphor screen is lens imaged onto a charge-coupled device camera for quantitative analysis.

The pulse-to-pulse heating laser fluctuation is within $\pm 10\%$. The spatial nonuniformity of the beam across the sample is controlled within $\pm 15\%$ by making the full width at half-maximum (FWHM) of the heating laser beam spatial profile on the surface more than the sample size. The heating laser pulse and the electron probe pulse are temporally synchronized on the surface of the sample. An optical delay line is used to set different delay times between the heating laser pulse and the electron probe pulse. This allows the RHEED patterns to be monitored throughout the laser-induced transient heating process. A total of 3000–5000 laser pulses are used to acquire each datum.

Germanium single-crystal wafers cut to $(111) \pm 0.2°$, $(110) \pm 0.3°$, and $(100) \pm 1°$ orientations are used. The Ge(111) and Ge(100) wafers are undoped with a resistivity of 42–45 Ohm cm and 47–55 Ohm cm, respectively. The Ge(110) wafers are *N*-type doped with resistivity in the 1.91 to 2.49 Ohm cm range. All the studied surfaces are polished for epitaxy ready by the manufacturer. The small miscut angles of the vicinal surfaces minimize effects caused by terraces, steps, and step edges. The sample is heated during the experiment by passing through it direct current. At the low-temperature range, the surface temperature is monitored by an *R*-type thermocouple pressed against the surface of the sample with an estimated uncertainty of ± 2 °C. At the high-temperature range, the surface temperature is measured with an infrared pyrometer, which is calibrated to the melting point of the bulk Ge using an emissivity of 0.46. The accuracy of the pyrometer measurement is estimated to be ± 10 °C. The time-resolved RHEED system is operated in ultrahigh vacuum operating in the low 10^{-10} Torr range. The samples are cleaned *in situ* by cycles of Ar^+ bombardment at about 500 °C followed by annealing at 700 °C for 10 to 30 minutes. The samples are always kept at 500 °C between experiments. An Auger analyzer is used to check surface cleanness before each experiment. No detectable impurities are observed during data acquisition.

The time-resolved RHEED system can also be operated at the continuous mode in which an UV lamp is used to illuminate the cathode of the photoactivated electron gun, producing a steady continuous electron beam. This mode of operation is used to characterize the temperature dependence of the surface structure. This temperature dependence of the RHEED intensity serves as a calibration for converting the time-resolved diffraction intensity to a transient surface temperature rise. For the experiments discussed here, the electron energy for the photoactivated RHEED gun operated in both pulsed and continuous mode is 21 keV.

III. EXPERIMENTAL RESULTS

A. Transient heating of germanium surfaces by 100 ps laser pulse

The transient temperature of the germanium surfaces heated by the laser pulses are obtained by monitoring the

RHEED streak intensity with time in the pump-probe setup and relating this to RHEED intensity with the surface temperature as measured for continuous heating.[37] In the case of 100-ps laser-pulsed heating, the rate of the surface temperature rise and decay is on the order of 10^{12} K/sec. The lattice vibration frequency is about 10^{13} per second, while the time duration (FWHM) of the probe electron beam in our time-resolved RHEED is ~100 ps. Therefore, the time-resolved RHEED intensity attenuation represents the dephasing effect of the thermal vibration due to the surface temperature increase when no phase transition occurs. As the first step to measure the transient surface temperature caused by the laser pulse, the RHEED intensity is calibrated to the static temperature measurements with the photoactivated electron gun operated in a continuous mode. In this case, an ultraviolet lamp is used in place of the pulsed-laser beam to illuminate the cathode of the photoactivated electron gun. The temperature dependence of the RHEED intensity is then used to obtain the transient surface temperature rise during laser-pulse heating.

The time-resolved RHEED intensity measurements are performed to determine the laser-induced transient temperature rise on the Ge(111) surface below the high-temperature phase transition.[38] The time-resolved RHEED intensity normalized to that at a base temperature is obtained for different delay times between the laser heating pulse and the electron probe pulse. The transient surface temperature rise can be extracted using the calibration of the temperature dependence of the RHEED intensity. The surface temperature rise is at its maximum at t_0 when the probe electron pulse arrives on the surface at a time near the end of the heating laser pulse, i.e., at maximum reduction in RHEED intensity. We have not included convolution effects due to the fact that the electron probe pulse width is comparable to the laser heating pulse width. These effects are small due to the relatively low thermal conductivity of Ge, thus, surface temperature decay time is much slower than the electron probe pulse width. The transient surface temperature rise is in good agreement with the classical heat-diffusion model.[39] This measurement is conducted with the sample kept at different base temperatures ranging from 300 to 910 K as shown in Fig. 2. We note that the effect of laser transient heating on the diffraction pattern is larger at the higher-base temperatures than for that at the lower-base temperatures when subjected to the same laser-peak fluence. This is due to the temperature dependence of the material parameters, especially the optical-absorption coefficient. As shown in Fig. 2, the maximum transient surface temperature rise at the base temperature of 830 K pumped by the same laser fluence increases two times more than that near room temperature, where the error bar indicates the nonuniformity of the laser-beam profile across the sample surface. For Ge(100) and Ge(110), the same measurements were performed to obtain the maximum transient surface temperature rise by heating with the laser pulse at high base temperatures. The results in Fig. 2, also show that the transient laser heating is independent of the surface orientation within the experimental error. This is in agreement with the classical heat diffusion model, since the material parameters, i.e., heat capacity, thermal conductivity, optical reflectivity, and optical-absorption coefficient do not vary much with the orientation.

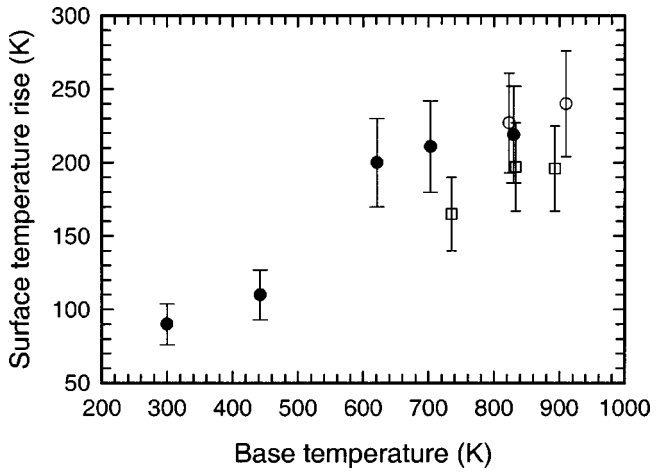

FIG. 2. Surface temperature rise at time t_0 corresponding to minimum RHEED intensity increases with base temperature for germanium surface. ●: Ge(111), □: Ge(100), ○: Ge(110). The heating laser-pulse peak fluence is kept constant at $1.8 \pm 0.27 \times 10^8$ W/cm^2. The error bars account for the nonuniformity of the heating laser fluence across the sample surface.

The maximum transient temperature rises on the germanium surfaces are related to the peak fluence of the heating laser pulse. This relation is used to determine the maximum surface temperature rise for a given laser-peak fluence. The maximum surface temperature rise is proportional to the laser peak fluence when the latent heat of the phase transition is negligible compared to the laser-pulse energy, which is the case for a surface phase transition. The surface temperature rise extracted from the time-resolved RHEED intensity is also lower than the actual value near the time at the maximum reduction of the RHEED intensity due to the convolution effect. This effect is caused by the fact that the electron probe pulse width is comparable to the laser heating pulse width. Ideally, the electron probe pulse width should be much less than the rise and decay times of surface temperature. For this temperature measurement, we are assuming that the carriers and phonons are both in equilibrium with themselves and with each other because of the relatively long time (>100 ps) considered in the present measurements. We next discuss the results obtained for each of the three studied surfaces.

B. Ge(111)

The temperature dependence of the Ge(111) surface properties near the Ge bulk melting temperature T_m has been the subject of several studies. An anomalous reduction of the sticking coefficient of O_2 on the Ge(111) surface was first observed by Lever at a temperature about 150 K below T_m.[40,41] This phenomenon was not observed on Ge(110) and Ge(100).[42] It was first proposed by Lever that this drop in the sticking coefficient is caused by a surface structural phase transition. In a low-energy electron diffraction (LEED) study, McRae and Malic reported that the intensities of the

surface diffraction peaks decrease rapidly near 1050 K and saturate at a low but nonzero value above 1050 K.[43,44] Their observation suggested that the outermost few atomic double layers lose lateral crystalline order in a continuous phase transition with a critical temperature T_c of about 1058 K. An ion-shadowing and blocking study using medium-energy ion scattering, which is sensitive to short-range order, concluded that 1–1.5 bilayers are positionally disordered at 1050 K.[45] The thickness of the disordered bilayers remains constant up to 25 K below T_m. The surface disorder transition observed on Ge(111) has been concluded to be a type of ''incomplete melting'' in which only the topmost bilayer on the Ge(111) surface melts during the order-disorder phase transition, and the thickness of this liquid bilayer remains constant up to T_m. Further experiments on the Ge(111) surface using electron energy-loss spectroscopy (EELS),[46] Ge $3p$ x-ray photoelectron diffraction and photoelectron holography,[47,48] have supported this incomplete melting model. On the other hand, a synchrotron x-ray diffraction study has observed a lack of surface roughening or surface melting, and suggested a proliferation of surface vacancies in the first bilayer with a vacancy concentration as high as 50%.[49] Using high-resolution helium scattering, Meli *et al.* suggested that the phase transition at about 1050 K is an order-order type with the bilayer spacing reduced by about 10% above T_c.[50]

Theoretical studies of the Ge(111) high-temperature phase transition concentrated on the first-principle molecular dynamic (MD) simulation.[51] In an MD simulation study of the Ge(111) surface within 2% of T_m, McRae *et al.*suggested that the long-range disordering occurs only laterally on the outermost bilayer while the layerlike ordering is maintained up to the outermost bilayer.[52] The MD simulation of Takeuchi, Selloni, and Tosatti has supported the incomplete melting model near T_m.[53] In this simulation, the disordering was found to be confined to the first atomic bilayer, and this disordered bilayer has a liquidlike diffusion and metallic characteristics as for liquid germanium. Two physical reasons have been postulated for the incomplete melting of a semiconductor surface such as Ge(111). A modified Landau theory was developed by Chernov and Mikheev considering the layering effect of a liquid layer in contact with the solid substrate.[54,55] When this model was applied to the Ge(111) surface, where the layering effect is prominent due to the stacking normal to the [111] direction, the surface was found to be stable with only the topmost layer melting at T_c.[45] An energy barrier was shown to exist in this phase transition that prevented the divergence of the liquid layer thickness. Another reason for incomplete melting of Ge(111) is based on surface metallization, which arises from the attraction between the semi-infinite semiconductor and a thin metallic film representing the top disordered layer. This attraction can stabilize the liquid film thickness limiting its thickness for Ge(111) to one bilayer up to T_m.[53]

Experimental results from low-energy electron diffraction, x-ray scattering, photoelectron diffraction, and helium scattering have been explained based on incomplete melting and metallization on the Ge(111) surface near T_m.[53] This incomplete melting of Ge(111), where a disordered film is formed at a critical temperature T_c of about 1050 K and the thickness of the film remains constant with increasing temperature, is different from the surface melting transition observed on open fcc metal surfaces, such as Pb(110) and Al(110), where the thickness of the disordered film diverges as the bulk melting temperature is approached.[28–31] Moreover, incomplete melting of the Ge(111) surface is also postulated to be different from incomplete melting or nonmelting of metal surfaces, due to the exchange correlation between the semi-infinite semiconducting germanium crystal and thin metallic liquid germanium layer.[56]

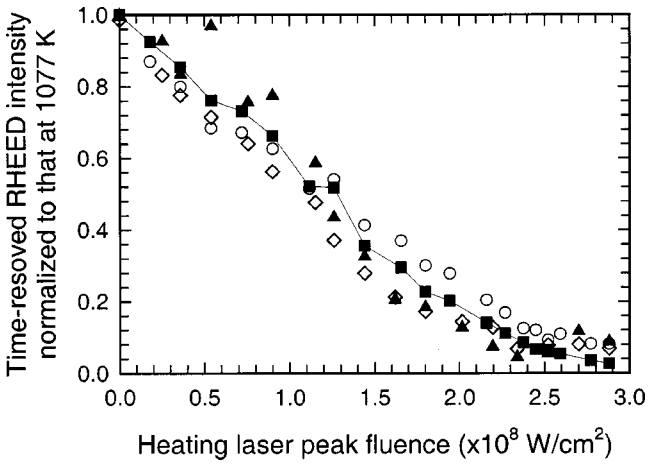

FIG. 3. Variation of the time-resolved Ge(111) RHEED intensity, normalized to that at a base temperature of 1077 K, with heating laser peak fluence. The diffraction intensity is obtained at time t_0 when the RHEED intensity is at its lowest point, which is near when the surface temperature is at its maximum. The electron beam angle of incidence is ~2.4°. ▲: (00) streak and ◇: (01) streak, the electron beam is incident along $[1\bar{1}0]$. ■: (00) streak and ○: (01) streak, the electron beam is incident along $[1\bar{2}1]$. The maximum temperature rise on the Ge(111) surface is found to be 219 ± 33 K for a laser peak fluence of $1.8\pm0.27\times10^8$ W/cm^2.

Previously,[38] we reported that the Ge(111) surface is overheated 63 ± 23 K beyond the temperature of the thermodynamic incomplete melting when subjected to 100-ps laser pulsed heating. At higher temperatures, the surface remains in the incomplete melting state in which only the topmost bilayer disorders with the presence of order in the second and deeper layers. Since our RHEED electron probe detects the top 2–3 atomic bilayers, the growth of the topmost liquid layer into the deeper layers could be observed. In order to investigate the stability of this incomplete melting state at high temperatures, even exceeding T_m, induced by 100-ps laser pulsed heating, time-resolved RHEED measurements are performed with the optical delay line set at the point of maximum reduction in the RHEED intensity t_0. The RHEED streak intensity, normalized to that at a given base temperature, is obtained for various laser peak fluences. The sample base temperature is kept at 1077 K. At this temperature, the incomplete melting is present on the Ge(111) surface. Results are shown in Fig. 3, which are obtained for the (00) and (01) RHEED streaks with the electron-beam incident along the $[1\bar{1}0]$ and $[1\bar{2}1]$ azimuths. It is shown in Fig. 3 that the Ge(111) surface retains the residual order up to a

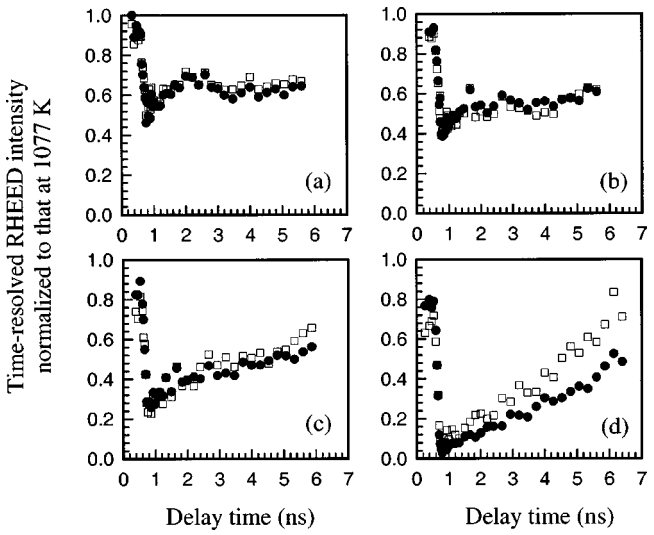

FIG. 4. Time-resolved normalized RHEED intensity [●: (00) streak, □: (01) streak] versus delay time between the electron probing pulse and the laser heating pulse with the Ge(111) surface subjected to different laser-peak fluences (I_p). The electron beam is incident along the $[1\bar{2}1]$ direction at an angle of ~2.4°. The Ge(111) surface is maintained at a base temperatures of 1077 K. (a) $I_p = 0.90 \pm 0.14 \times 10^8$ W/cm^2; (b) $I_p = 1.26 \pm 0.19 \times 10^8$ W/cm^2; (c) $I_p = 1.98 \pm 0.30 \times 10^8$ W/cm^2; (d) $I_p = 2.88 \pm 0.43 \times 10^8$ W/cm^2.

laser peak fluence of $(2.2 \pm 0.3) \times 10^8$ W/cm^2 corresponding to a maximum surface temperature of 1344 ± 40 K, where the maximum transient surface temperature rise was obtained for the corresponding laser peak fluence using Fig. 2 with a base temperature of 830 K. The obtained maximum surface temperature rise is lower than the actual value due to convolution effect and the higher base temperature in Fig. 3 (1077 K). This indicates the stability of the incomplete melting state of Ge(111) surface at 134 ± 40 K beyond the bulk melting point (1210 K). The indicated errors are due to the nonuniformity of the laser beam across the probed sample area. Above $(2.2 \pm 0.3) \times 10^8$ W/cm^2, the RHEED intensity was observed to disappear into the background due to incomplete melting growing vertically into layers under the top atomic bilayer of the Ge(111) surface.

Further experiments are performed to examine the temporal behavior of the growth of melting. In these experiments, the normalized RHEED streak intensities are obtained at various delay times between the laser heating pulse and the electron probe pulse. Time-resolved RHEED intensity of the (00) and (01) streaks for different incident laser peak fluences are shown in Figs. 4(a)–4(d). The base temperature of the surface is 1077 K. For these measurements, the maximum transient surface temperature rise is related to the corresponding laser peak fluence using Fig. 2, obtained for a base temperature of 830 K. In Figs. 4(a)–4(c), the sample is heated to a maximum surface temperature of 1186 ± 17, 1230 ± 23, and 1317 ± 36 K, when subjected to a laser peak fluence of $0.90 \pm 0.14 \times 10^8$, $1.26 \pm 0.19 \times 10^8$, and $1.98 \pm 0.30 \times 10^8$ W/cm^2 across the probed sample area, respectively. For these cases, the experimental data show qualitative agreement with what is expected from heat diffusion; a rapid decrease in the normalized streak intensity followed by an increase as the heat is conducted to the bulk.

In Fig. 4(d), a laser peak fluence sufficient to heat the Ge(111) surface to a maximum surface temperature of 1427 ± 53 K is used. This temperature is above the maximum superheating temperature of 1344 ± 40 K observed for the Ge(111) surface covered with an incomplete molten layer when subjected to 100-ps laser heating pulse. For this set, the time-resolved RHEED intensity shows an initial fast decrease down to the background intensity level within about 200 ps. The RHEED intensity remains at a background level for about 0.5 ns, indicating the melting duration of the surface into deeper layers. The RHEED intensity is observed to increase back slowly indicating the start of the surface recrystallization during cooling by heat diffusion into the bulk. In all of the experiments reported here, no permanent damage is observed on the surface, and the surface recovers to its initial condition following the laser pulse. All experiments are conducted at a 50 Hz repetition rate.

Therefore, we conclude that the Ge(111) incomplete surface melting state superheats and remains stable up to at least $T_m + 134 \pm 40$ K. In this superheated state the top quasiliquid bilayer on the Ge(111) surface remains stable when heated by 100-ps laser pulses and do not propagate deeper. For laser fluences raising the surface temperature above that maximum stability temperature, melting propagates into deeper layers. The superheating of the Ge(111) incomplete melting state could be attributed to the metallization of the top bilayer leading to interaction between the top metallic bi-layer and the semi-infinite semiconductor underneath stabilizing the liquid film as proposed by Takeuchi, Selloni and Tosatti.[53] Another form of an energy barrier for melting, such as a strong layering effect on the topmost atomic 1–2 bilayer, might be involved.[45] However, this later mechanism was ruled out by Takeuchi, Selloni and Tosatti as a possible explanation for the incomplete melting transition on Ge(111) under slow equilibrium heating conditions.[53]

C. Ge(100)

The next surface we have studied is Ge(100). The Ge(100) surface is characterized by a strong short-range reconstruction with a weaker long-range ordering across the domains. The termination of the bulk lattice of Ge(100) leaves two dangling bonds-per-surface atom. This leads to the formation of rows of buckled and asymmetric dimers that minimize the surface free energy.[57–59] The dimerization results in a (2×1) reconstruction at the surface. Two 2×1 domains rotated by 90°, are generally observed. Regions of local 2×1 and $c(4 \times 2)$ and $p(2 \times 2)$ symmetry are also observed.[58] Surface x-ray diffraction measurements show that the reconstructed Ge(100) surface undergoes a reversible $(2 \times 1) \Leftrightarrow (1 \times 1)$ phase transition at $T_c = 955$ K.[60] There are two conflicting models proposed on the nature of this surface phase transition. The first model was proposed by Johnson *et al.* who suggested that this phase transition is accompanied with adatom-vacancy creation and dimer break-up on the Ge(100) surface.[60] The adatom-vacancy creation during the phase transition is supported by the change of the

integrated intensity of the fractional order beams of X-ray diffraction during the phase transition and the observation that the FWHM of fractional order beams remain the same up to T_c of the phase transition. At temperatures above 980 K the specular intensity of X-ray diffraction was shown to saturate to the background. This behavior was shown to be reversible if the maximum temperature was kept below 1020 K.[60] If the surface was taken above this temperature, a significant increase in surface roughening was observed as indicated by the rapid drop in the reflected intensity.

This observed surface-roughening behavior is different from surface melting observed on metal surfaces for which the surface order changes continuously across the transition.[28–31] Thus, the X-ray study of the Ge(100)-$(2\times1)-(1\times1)$ phase transition excludes domain size reduction caused by the creation of steps or the domain-wall movement during the surface phase transition. It was concluded from X-ray diffraction that the $(2\times1)-(1\times1)$ phase transition involves an assisted breakup of dimers with some vertical atomic movement.[60] Since the low-temperature stability of the Ge(100) surface is due to partially accommodating of dangling bonds by the reconstruction forming dimers, it is not surprising that surface roughening is accompanied with disappearance of the reconstruction. As the surface becomes increasingly more disordered, the average number of dimers destroyed per newly formed adatom-vacancy pair falls. The defects form the nuclei for further disordering, since locally, the energy penalty for disordering is lowered. Thus, the Ge(100)-$(2\times1)-(1\times1)$ phase transition accelerates as a function of temperature and the fractional order intensity of x-ray diffraction was observed to drop precipitously. The surface becomes further roughened above 980 K where the roughening involves step creation and movement.[60]

The second model describes the nature of the phase transition as domain-wall movement with the number of dimers conserved during the phase transition. The adatom-vacancy proliferation during the phase transition was first questioned by a He-atom scattering study, where the domain-wall proliferation was observed.[61] Moreover, the dimer breakup model was rejected based on an extended spectroscopic study of the Ge three-dimensional (3D) surface core-level shift. This study showed conservation of the total number of dimers through both the $c(4\times2)-(2\times1)$ and $(2\times1)-(1\times1)$ surface phase transitions up to 1143 K.[62–64] Therefore, these experiments suggested the (2×1) domain-wall proliferation instead of dimer breakup during the high-temperature phase transition at 950 K with an order-disorder character. The (2×1) long-range order is gradually lost as the domain walls start to proliferate. An increase in the step density was also observed from the broadening of the He-atom specular (00) beam. Step creation was shown to be only partially involved in the disordering of the (2×1) phase.[65] At temperature higher than the Ge(100)-$(2\times1)-(1\times1)$ phase transition, another phase transition was reported from valence-band photoemission study, where a discontinuity in the emission intensity at Fermi level was observed.[64]

In order to investigate the stability of the Ge(100) surface at high temperature for 100-ps laser pulsed heating, time-resolved RHEED measurements were performed with the optical delay line set at t_0. The RHEED streak intensity, normalized to that at a given base temperature, is obtained for various laser peak fluences. Results are shown in Fig. 5 for two pump-probe scans with base temperatures of 893 and 983 K, which are obtained for the (00) and (01) RHEED streaks with the electron-beam incident along the [011] azimuth. It is shown in Figs. 5(a) and 5(b) that the Ge(100) surface melts at laser peak fluences of $2.4\pm0.4\times10^8$ and $1.6\pm0.3\times10^8$ W/cm^2 corresponding to maximum surface temperatures of 1154 ± 39 and 1156 ± 26 K, respectively. The maximum transient surface temperature rises are obtained for the corresponding laser peak fluences using Fig. 2 for Ge(100) with the base temperatures of 893 and 983 K. The indicated errors are only due to the nonuniformity of the laser beam across the probed surface area. For these two sets, the Ge(100) surface disorders near the bulk melting point when subjected to 100-ps laser pulsed heating. The experimental error in this data set, convolution effect due to electron-beam pulse width, and the low RHEED intensity due to the proliferation of vacancies do not allow us to conclusively determine the melting point of the Ge(100) surface. However, the results favor the lack superheating, in contrast to the Ge(111) surface for which superheating is clearly observed. Although the temperature reported above for the disappearance of the diffraction pattern is below the bulk melting point, we point that convolution effects and the higher base temperature than that for the calibration in Fig. 2 results in a higher transient surface temperature. In addition, the high RHEED background makes it difficult to detect any long-range surface order. Thus, the melting temperature is expected to be higher than that mentioned above and is probably at or close to T_m. Surface complete melting of semiconductors are assumed to be energetically disallowed because of the negative Hamaker constant.[53,66]

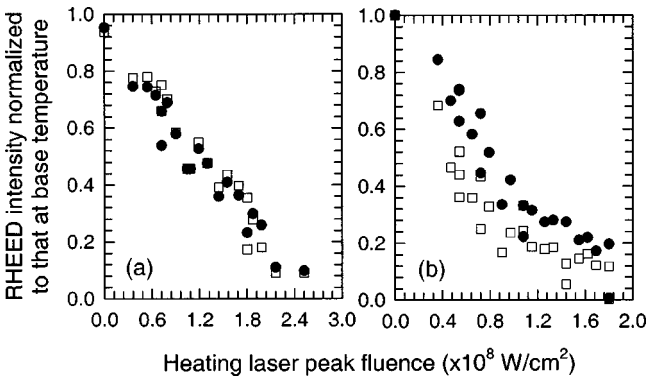

FIG. 5. Time-resolved RHEED intensity [●: (00) streak, □: (01) streak] normalized to that at base temperature for different heating laser-peak fluences for Ge(100). The electron beam is incident along the [011] direction at an angle of ~2°. (a) Base temperature=893 K; (b) Base temperature=983 K. The RHEED intensities are obtained at the time t_0.

Further experiments were performed to examine the temporal behavior of the melting process. In these experiments, normalized RHEED streak intensities were obtained at various delay times between the laser heating pulse and the elec-

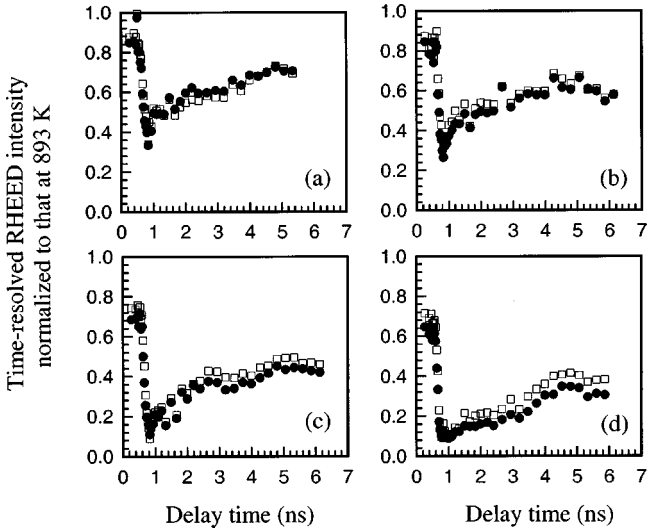

FIG. 6. Time-resolved normalized RHEED intensity [●: (00) streak, □: (01) streak] versus delay time between the electron probing pulse and the laser heating pulse for Ge(100) subjected to different laser-peak fluences (I_p). The electron beam is incident along the [011] direction at an angle of ~2°. The Ge(100) surface is maintained at a base temperatures of 893 K. (a) $I_p = 1.08 \pm 0.16 \times 10^8$ W/cm^2; (b) $I_p = 1.44 \pm 0.22 \times 10^8$ W/cm^2; (c) $I_p = 2.16 \pm 0.32 \times 10^8$ W/cm^2; (d) $I_p = 2.52 \pm 0.38 \times 10^8$ W/cm^2.

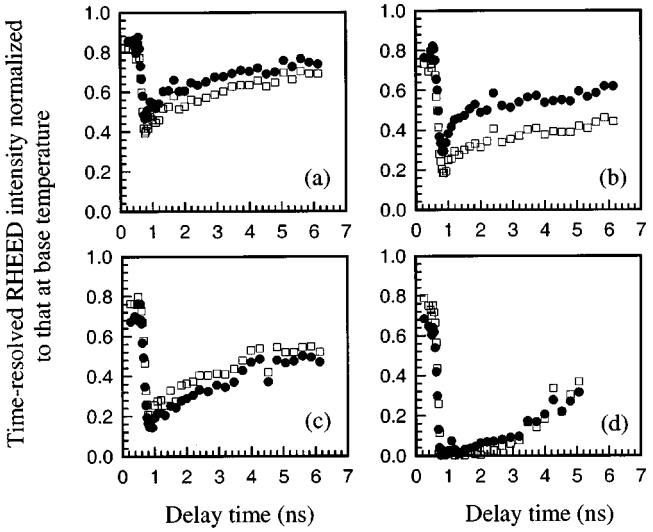

FIG. 7. Time-resolved normalized RHEED intensity [●: (00) streak, □: (01) streak] versus delay time between the electron probing pulse and the laser heating pulse with the Ge(100) surface subjected to a laser-peak fluence (I_p) of $1.8 \pm 0.27 \times 10^8$ W/cm^2 with different base temperatures. (a) 735 K; (b) 833 K; (c) 893 K; (d) 983 K. The electron beam is incident along [011] at an angle of ~2°.

tron probe pulse. Results for different incident laser peak fluences are shown in Fig. 6. The sample base temperature is kept at 893 K. For these measurements, the maximum transient surface temperature rises are related to the corresponding laser peak fluences using Fig. 2 for Ge(100) with the base temperature of 893 K. In Figs. 6(a)–6(c), the sample is heated to a maximum surface temperature of 1011 ± 18, 1050 ± 24, and 1128 ± 35 K, when subjected to laser peak fluences of $(1.08 \pm 0.16) \times 10^8$, $(1.44 \pm 0.22) \times 10^8$, and $(2.16 \pm 0.32) \times 10^8$ W/cm^2 across the probed surface area, respectively. For these cases, the experimental data agree with the expected trends for heat diffusion: a rapid decrease in the normalized streak intensity followed by an increase as the heat is conducted into the bulk.

In Fig. 6(d), a laser peak fluence of $(2.52 \pm 0.38) \times 10^8$ is sufficient to heat the sample to a maximum surface temperature of 1172 ± 42 K. For this set, the time-resolved RHEED intensity shows an initial fast decrease down to almost background level within ~200 ps. This remains for ~0.5 ns, which is interpreted as the melting duration of the Ge(100) surface. After that, the RHEED intensity increases back slowly indicating the appearance of surface long-range order during cooling by heat diffusion to the bulk.

In another set of experiments, the laser peak fluence is fixed at $1.8 \pm 0.27 \times 10^8$ W/cm^2 while the base temperature is varied. The results are shown in Figs. 7(a)–7(d) for base temperature of 735, 833, 893, and 983 K, respectively. In Figs. 7(a)–7(c), the maximum transient temperatures are 900 ± 25, 1029 ± 29, and 1088 ± 29 K, which are obtained from Fig. 2 for Ge(100) with the corresponding base temperature. For these sets of measurements, the surface is observed to remain in order. In Fig. 7(d), the maximum transient temperature is 1179 ± 29 K, which is obtained from Fig. 2 for Ge(100) with base temperature of 893 K. As mentioned before, the actual maximum transient temperature is expected to be higher than that due to the convolution effect and the higher base temperature than that for the calibration. The normalized RHEED intensity is observed to remain within the background level for ~3 ns followed by a slow recovery indicating recrystallization due to heat conduction to the bulk. For this measurement, the surface is observed to melt near the bulk melting temperature when subjected to 100-ps laser-pulsed heating. The data favor the view that no residual order is present above the bulk melting point for the Ge(100) surface.

In summary, the time-resolved RHEED results show that the Ge(100) surface melts near the bulk melting point T_m for transient heating with 100-ps laser pulse in contrast to the superheating of the Ge(111) surface. The experimental error, convolution effect, and low RHEED intensity because of the proliferation of vacancies do not allow us to conclusively determine the melting point of Ge(100) under transient laser heating. However, the results favor the lack of superheating of the Ge(100) surface and show a strong contrast between transient melting behavior of the Ge(111) and Ge(100) surfaces.

D. Ge(110)

The final surface considered is Ge(110). Of the three low-index surfaces of germanium, the Ge(110) surface is by far the least studied. From studies of valence band and Ge 3D core-level photoemissions, a surface phase transition has been observed with a weak surface metallization at 800 K.[67,68] This metallic behavior of the surface was found to

increase continuously up to 1110 K. An abrupt and intense jump of the photoemission intensity at Fermi level was also observed at 1110 K.[67] This discontinuity in the photoemission intensity was attributed either to a further breakdown of surface atomic bonds or to the onset of an incomplete melting phase transition at 1110 K similar to the reported behavior of the adatom-restatom of Ge(111).

Reconstruction on the Ge(110) surface shows uncommon features: a $c(8\times10)$ structure appears at temperatures below 650 K, a 2×16 superstructure is observed at the temperatures above 650 and below 700 K, reappearance of the $c(8\times10)$ structure is obtained above 700 K.[69–71] These reconstructions are identified to be formed by adatoms. Ideally terminated Ge(110) exposes zigzag atomic rows along the $[1\bar{1}0]$ direction with second-layer zigzag rows displaced relatively by half spacing to the first layer. Each atom at the first layer has one dangling bond. At temperatures below 650 K, the surface free energy was shown to minimize locally with adatoms forming zigzag trains of polygons along the $[2\bar{2}5]$ direction. The trains are thought to run along the $[2\bar{2}5]$ direction as well. The adatom polygons were found to have symmetry of a ''centered'' 8×10 periodicity, with the sides of the unit mesh along the $[1\bar{1}0]$ and [001] directions.[69–71] The Ge(110)-$c(8\times10)$ reconstruction was observed by LEED, RHEED, and scanning tunneling microscopy (STM).[69–71] Ge(110)-2×16 reconstruction was observed using STM after surface cooling to 700 K from an annealing temperature of 1000 K.[70] Noro and Ichikawa proposed a model for the Ge(110)-2×16 reconstruction, where the surface consists of a periodic up-and-down sequence of terraces with a height difference of an [110] plane spacing.[69] In their model, the parallel terrace steps are along the $[1\bar{1}2]$ direction. Zigzag adatom chains are formed on the terraces with the chains running along the $[1\bar{1}2]$ direction. The unit mesh of the adatom chains has a translational symmetry of 2×16 as for Si(110).[69] The $c(8\times10)$ reconstruction has been observed to reappear above 700 K with the fractional order in RHEED patterns becoming less defined with increasing temperature and fading in the high background above 800 K.[69] Ge 3D core-level photoemission study of Ge(110) at high temperature has suggested a metallic surface character above 750 K.[67]

In order to investigate the structural stability of the Ge(110) surface at a high temperature induced by 100-ps laser-pulsed heating, time-resolved RHEED measurements were performed with the optical delay line set at t_0 similar to measurements conducted on Ge(111) and Ge(100). The RHEED streak intensity, normalized to that at a given base temperature, is obtained for various laser peak fluences. Results are shown in Fig. 8 for two pump-probe scans with base temperatures of 1003 and 1080 K and obtained for the (00) and (11) RHEED streaks. The electron beam is incident along the $[\bar{1}12]$ azimuth. It is shown in Fig. 8 that the Ge(110) surface melts at laser peak fluences of $(1.40\pm0.21)\times10^8$ and $(0.80\pm0.12)\times10^8$ W/cm^2 for the two different base temperatures that gives a maximum surface temperature of 1189 ± 28 and 1187 ± 16 K, respectively. The

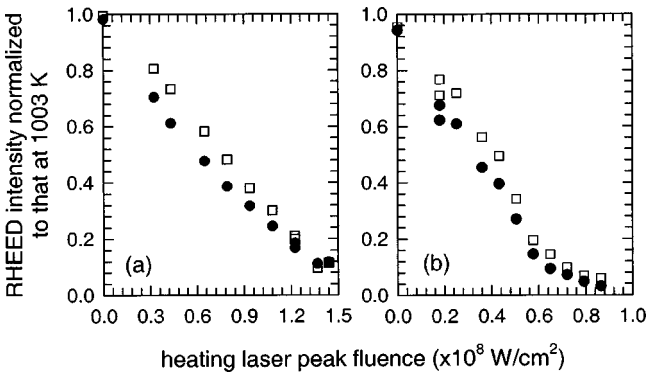

FIG. 8. Time-resolved RHEED intensity [●: (00) streak, □: (11) streak] for Ge(110) normalized to that at base temperature versus laser-peak fluence. (a) Base temperature=1003 K; (b) Base temperature=1080 K. RHEED intensities are obtained at the time t_0. The electron beam is incident along the $[\bar{1}12]$ direction at an angle of ~2°.

maximum transient surface temperature rises were obtained for the corresponding laser peak fluences using Fig. 2 for Ge(110) with a base temperature of 910 K. For these two sets, the Ge(110) surface melts near the bulk melting point ($T_m=1210$ K) when subjected to 100-ps laser heating. Convolution effects and using the calibration in Fig. 2 obtained at a temperature lower than the sample-base temperature result in underestimating the maximum transient surface temperature as described before.

Further experiments were performed to examine the temporal behavior of the melting of Ge(110). In these experiments, normalized RHEED streak intensities were obtained at various delay times between the laser heating pulse and the electron probe pulse. Results for different incident laser peak fluences are shown in Fig. 9. The sample base temperature is kept at 1003 and 1080 K. For these measurements, the maximum transient surface temperature rises are related to the corresponding laser peak fluences using Fig. 2 for Ge(110) with a base temperature of 910 K. In Figs. 9(a) and 9(c), the sample is heated to a maximum surface temperature of 1147 ± 22 and 1128 ± 7 K, when subjected to a laser peak fluence of $(1.08\pm0.16)\times10^8$ and $(0.36\pm0.06)\times10^8$ W/cm^2 over the probed surface area, respectively. For these two cases, the experimental data agree with that expected from the classical heat diffusion: a rapid decrease in the normalized streak intensity followed by an increase as the heat is conducted into the bulk. For Fig. 9(b) the sample is heated to a maximum transient temperature of 1195 ± 29 K by a laser peak fluence of $(1.44\pm0.22)\times10^8$ W/cm^2. In this case, the maximum transient surface temperature is just enough to cause surface melting.

In Fig. 9(d), a sufficient laser fluence of $(0.72\pm0.11)\times10^8$ W/cm^2 is provided to heat the sample to a maximum surface temperature of 1176 ± 14 K, according to the RHEED measurement. If the convolution effect and the high base temperature are considered, this maximum surface temperature jump could be closer to the bulk melting point, $T_m=1210$ K. The lower-transient temperature rise obtained in Fig. 9(d) than that obtained in Fig. 9(b) is attributed to the

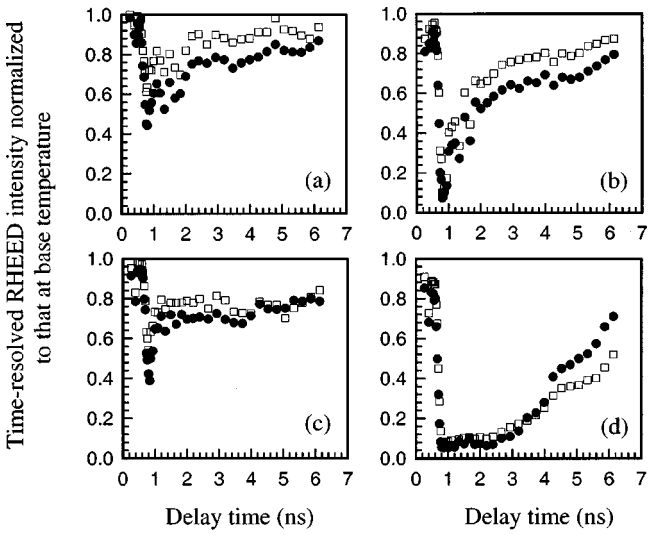

FIG. 9. Time-resolved normalized RHEED intensity [●: (00) streak, □: (11) streak] versus delay time between the electron probing pulse and the laser heating pulse with Ge(110) maintained at two different base temperatures and subjected to different laser-peak fluences (I_p). The electron beam is incident along the [$\bar{1}\bar{1}2$] direction at an angle of ~2°. (a) $I_p=(1.08\pm0.16)\times10^8$ W/cm^2, base temperature=1003 K; (b) $I_p=1.44\pm0.22\times10^8$ W/cm^2, base temperature=1003 K; (c) $I_p=0.36\pm0.06\times10^8$ W/cm^2, base temperature=1080 K; (d) $I_p=0.72\pm0.11\times10^8$ W/cm^2, base temperature=1080 K.

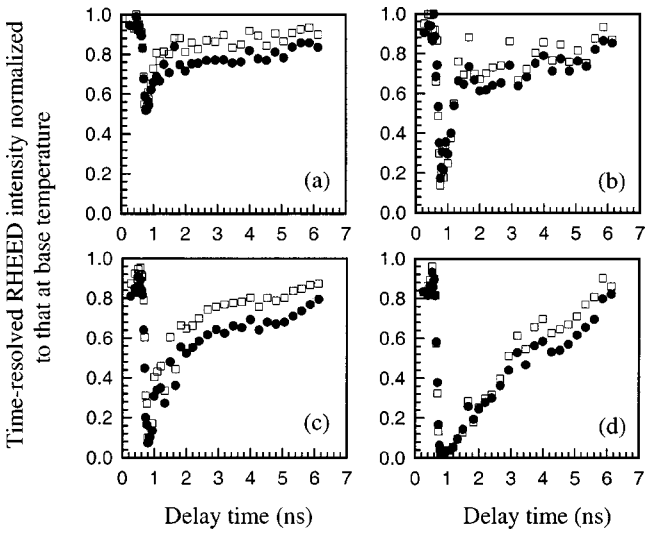

FIG. 10. Time-resolved normalized RHEED intensity [●: (00) streak, □: (11) streak] versus delay time between the electron probing pulse and the laser heating pulse. The Ge(110) surface is subjected to a laser peak fluence (I_p) of $1.8\pm0.27\times10^8$ W/cm^2 except for (c) and the surface is maintained at different base temperatures. (a) 823 K; (b) 910 K; (c) 1003 K ($I_p=1.44\pm0.22\times10^8$ W/cm^2); (d) 1009 K. The electron beam is incident along the [$\bar{1}\bar{1}2$] direction at an angle of ~2°.

higher base temperature in Fig. 9(d). For this case, the time-resolved RHEED intensity shows an initial fast decrease down to the background level within about 200 ps, followed by ~1.5 ns with the RHEED intensity remaining within the background indicating the melting duration of the surface. Subsequently, the RHEED intensity increases back slowly indicating the start of the surface recrystallization during cooling by heat diffusion to the bulk.

In another set of experiments shown in Figs. 10(a)–10(d), the laser peak fluence is fixed at $(1.8\pm0.27)\times10^8$ W/cm^2 [$(1.44\pm0.22)\times10^8$ W/cm^2 for (c)] while the base temperature is varied. In Figs. 10(a)–10(c), the resulting maximum transient temperatures are 1019 ± 29, 1106 ± 29, 1160 ± 24 K, below the bulk melting point. For these sets, the experimental data agree with classical heat diffusion. For Fig. 10(d), the maximum transient temperature is 1205 ± 29 K, which is very close to the bulk melting point. This obtained value is the low limit due to the convolution effect and the higher base temperature than that used in the calibration curve of Fig. 2. In this case, the normalized RHEED intensity remains zero for ~0.5 ns followed by slow recovery indicating recrystallization due to heat conduction to the bulk. In all of the experiments reported here, no permanent surface damage is observed on the sample, and the surface recovers to its initial condition before the next laser pulse.

In conclusion, the time-resolved RHEED results show that the Ge(110) surface melts near the bulk melting point by transient heating using 100-ps laser pulses. Although the exact melting temperature of Ge(110) by 100-ps laser pulse heating cannot be conclusively concluded from the data due to the convolution effect and other experimental errors in the time-resolved RHEED, the results favor the conclusion that no residual order is retained on the Ge(110) surface significantly above the bulk melting temperature. These results are in contrast to the observation of clear superheating of the Ge(111) surface under similar heating conditions.

IV. SUMMARY

In summary, we have investigated the structural behavior of the three low-index surfaces of germanium at high temperatures near its bulk melting point using 100-ps time-resolved RHEED. Our time-resolved measurements show that the incomplete melting state of the Ge(111) surface remains stable at least up to 1344 ± 40 K, which indicates the superheating of the incomplete melted Ge(111) surface beyond the bulk melting point by at least 134 ± 40 K under such transient heating conditions. For Ge(110) and Ge(100), melting near the bulk melting point is observed when the two surfaces are heated by 100-ps laser pulse. Because of the low-diffraction intensity at high temperatures and the temperature uncertainty in the time-resolved experiments, we are unable to conclusively determine the melting point of these surfaces in relation to the bulk melting point T_m under such transient heating. The results, however, favor lack of surface superheating of Ge(100) and, to some extent, of Ge(110) and show clear difference in the high temperature transient structural stability of Ge(111) when compared to Ge(100) and Ge(110). This prominent difference in the structural stability between Ge(111) surface and the Ge(100) and Ge(110) surfaces may be attributed to the metallization of the top bilayer of Ge(111) leading to interaction between the top metallic

bilayer and the semi-infinite semiconductor underneath stabilizing the liquid film as proposed by Takeuchi *et al.*[53] Other forms of energy barrier for melting such as strong layering effect on the topmost atomic 1–2 bilayer may also be involved.[45] This result extends our previous work on the orientation dependent structural stability of fcc metals, which showed that Pb(111) superheated while Pb(110) premelted under transient heating conditions similar to those used in the present study.[26] The present paper also indicates that it is possible to transiently superheat a surface with a quasimolten layer that does not propagate, in part, due to surface metallization or strong layering effects. For the reported experiments on Ge(111), the base temperature before pulsed laser heating was 1077 K at which only one surface bilayer is melted. If we take the view that metallization of the top bilayer and its interaction with the layers underneath prevents the growth of this liquid layer up to T_m for slow heating, then this mechanism of attraction could explain superheating under fast heating rates. Thus, the observed superheated state can be viewed as a metastable state occurring due to an energy barrier for growth of the quasimelted surface bilayer. This is not the case for the Ge(100) and Ge(110) surfaces for which the results indicate lack of any measurable surface superheating.

ACKNOWLEDGMENTS

The authors gratefully acknowledge B. Lin, I. El-Kholy, and M. Hegazy for their contributions in the experiments. This work was supported by the US Department of Energy, Division of Material Sciences, under Grant No. DE-FG02-97ER45625 and the National Science Foundation Grant No. DMR-9988669.

*Corresponding author. Email address: helsayed@odu.edu, FAX: (757) 683-3220.

[1] P. Stoltze, J. K. Nørskov, and U. Landman, Phys. Rev. Lett. **61**, 440 (1988).
[2] P. Stoltze, J. K. Nørskov, and U. Landman, Surf. Sci. **220**, L693 (1989).
[3] P. Stoltze, J. Chem. Phys. **92**, 6306 (1990).
[4] J. Mei and J. W. Davenport, Phys. Rev. B **46**, 21 (1992).
[5] P. Carnevali, F. Ercolessi, and E. Tosatti, Phys. Rev. B **36**, 6701 (1987).
[6] P. Carnevali, F. Ercolessi, and E. Tosatti, Surf. Sci. **189/190**, 645 (1987).
[7] F. Ercolessi, S. Iarlori, O. Tomagnini, E. Tosatti, and X. J. Chen, Surf. Sci. **251/252**, 645 (1991).
[8] F. Ercolessi, S. Iarlori, O. Tomagnini, and E. Tosatti, in *Nanosources and Manipulation of Atoms in High Fields and Temperatures: Applications*, Vol. 235 of NATO Advanced Study Institute, Series E: Applied Sciences, edited by Vu Thien Binh, N. Garcia, and K. Dransfeld (Kluwer Academic, Dordrecht, 1993).
[9] G. Bilalbegović, F. Ercolessi, and E. Tosatti, Surf. Sci. Lett. **258**, L676 (1991).
[10] G. Bilalbegović, F. Ercolessi, and E. Tosatti, Europhys. Lett. **18**, 163 (1992).
[11] G. Bilalbegović, F. Ercolessi, and E. Tosatti, Surf. Sci. **280**, 335 (1993).
[12] J. F. Lutsko, D. Wolf, S. R. Philipot, and S. Yip, Phys. Rev. B **40**, 2841 (1989).
[13] R. N. Barnett and U. Landman, Phys. Rev. B **44**, 3226 (1991).
[14] P. D. Ditlevsen, P. Stoltze, and J. K. Nørskov, Phys. Rev. B **44**, 13 002 (1991).
[15] B. Loisel, J. Lapujoulade, and V. Pontikis, Surf. Sci. **256**, 242 (1991).
[16] H. Häkkinen and M. Manninen, Phys. Rev. B **46**, 1725 (1992).
[17] H. Häkkinen and U. Landman, Phys. Rev. Lett. **71**, 1023 (1993).
[18] E. T. Chen, R. N. Barnett, and U. Landman, Phys. Rev. B **40**, 924 (1989).
[19] E. T. Chen, R. N. Barnett, and U. Landman, Phys. Rev. B **41**, 439 (1990).
[20] G. Bilalbegović, F. Ercolessi, and E. Tosatti, Europhys. Lett. **17**, 333 (1992).
[21] D. P. Woodruff, *The Solid Liquid Interface*, (Cambridge University, London, 1973).
[22] J. W. Herman and H. E. Elsayed-Ali, Phys. Rev. Lett. **68**, 2952 (1992).
[23] J. W. Herman and H. E. Elsayed-Ali, Phys. Rev. Lett. **69**, 1228 (1992).
[24] J. W. Herman, H. E. Elsayed-Ali, and E. A. Murphy, Phys. Rev. Lett. **71**, 400 (1993).
[25] E. A. Murphy, H. E. Elsayed-Ali, and J. W. Herman, Phys. Rev. B **48**, 4921 (1993).
[26] J. W. Herman and H. E. Elsayed-Ali, Phys. Rev. B **49**, 4886 (1994).
[27] F. D. Di Tolla, F. Ercolessi, and E. Tosatti, Phys. Rev. Lett. **74**, 3201 (1995).
[28] J. W. M. Frenken and J. F. van der Veen, Phys. Rev. Lett. **54**, 134 (1985).
[29] J. W. M. Frenken, P. M. J. Maree, and J. F. van der Veen, Phys. Rev. B **34**, 7506 (1986).
[30] B. Pluis, A. W. Denier van der Gon, J. W. M. Frenken, and J. F. van der Veen, Phys. Rev. Lett. **59**, 2678 (1987).
[31] A. W. Denier van der Gon, R. J. Smith, J. M. Gay, D. J. O'Connor, and J. F. van der Veen, Surf. Sci. **227**, 143 (1990).
[32] J. F. van der Veen, B. Pluis, and A. W. Denier van der Gon, in *Chemistry and Physics of Solid Surfaces VII*, Springer Series in Surface Science, Vol. 10, edited by R. Vanselow and R. F. Howe, (Springer-Verlag, Berlin, 1988), p. 455.
[33] J. C. Heyraud and J. J. Métois, Surf. Sci. **128**, 334 (1983).
[34] R. S. Becker, J. A. Golovchenko, and B. S. Swartzentruber, Phys. Rev. Lett. **54**, 2678 (1985).
[35] H. E. Elsayed-Ali and G. A. Mourou, Appl. Phys. Lett. **52**, 103 (1988).
[36] H. E. Elsayed-Ali and J. W. Herman, Rev. Sci. Instrum. **61**, 1636 (1990).
[37] H. E. Elsayed-Ali, J. Appl. Phys. **79**, 6853 (1996).
[38] Xinglin Zeng, Bo Lin, Ibrahim El-Kholy, and H. E. Elsayed-Ali, Surf. Sci. **439**, 95 (1999).
[39] Xinglin Zeng, Bo Lin, Ibrahim El-Kholy, and H. E. Elsayed-Ali, Phys. Rev. B **59**, 14 907 (1999).
[40] R. F. Lever, Surf. Sci. **9**, 370 (1968).
[41] R. F. Lever and H. R. Went, Surf. Sci. **19**, 435 (1970).

[42] A. A. Frantsuzov and N. I. Makrushin, Surf. Sci. **40**, 320 (1973).
[43] E. G. McRae and R. A. Malic, Phys. Rev. B **38**, 13 163 (1988).
[44] E. G. McRae and R. A. Malic, Phys. Rev. Lett. **58**, 1437 (1987).
[45] A. W. Denier van der Gon, J. M. Gay, J. W. M. Frenken, and J. F. van der Veen, Surf. Sci. **241**, 335 (1991).
[46] S. Modesti, V. R. Dhanak, M. Sancrotti, A. Santoni, B. N. J. Persson, and E. Tosatti, Phys. Rev. Lett. **73**, 1951 (1994).
[47] T. T. Tran, S. Thevuthasan, Y. J. Kim, D. J. Friedman, A. P. Kaduwela, G. S. Herman, and C. S. Fadley, Surf. Sci. **281**, 270 (1993).
[48] T. T. Tran, S. Thevuthasan, Y. J. Kim, G. S. Herman, D. J. Friedman, and C. S. Fadley, Phys. Rev. B **45**, 12 106 (1992).
[49] A. Mak, K. W. Evans-Lutterodt, K. Blum, D. Y. Noh, J. D. Brock, G. A. Held, and R. J. Birgeneau, Phys. Rev. Lett. **66**, 2002 (1991).
[50] C. A. Meli, E. F. Greene, G. Lange, and J. P. Toennies, Phys. Rev. Lett. **74**, 2054 (1995).
[51] R. Car and M. Parrinello, Phys. Rev. Lett. **55**, 2471 (1985).
[52] E. G. McRae, J. M. Landwehr, J. E. McRae, G. H. Gilmer, and M. H. Grabow, Phys. Rev. B **38**, 13 178 (1988).
[53] Noboru Takeuchi, A. Selloni, and E. Tosatti, Phys. Rev. Lett. **72**, 2227 (1994).
[54] A. A. Chernov and L. V. Mikheev, Phys. Rev. Lett. **60**, 2488 (1988).
[55] A. A. Chernov and L. V. Mikheev, Physica A **157**, 1042 (1989).
[56] G. Bilalbegović and E. Tosatti, Phys. Rev. B **48**, 11 240 (1993).
[57] D. J. Chadi, Phys. Rev. Lett. **43**, 43 (1979).
[58] J. A. Kubby, J. E. Griffith, R. S. Becker, and J. S. Vickers, Phys. Rev. B **36**, 6079 (1987).
[59] R. Rossmann, H. L. Meyerheim, V. Jahns, J. Wever, W. Moritz, D. Wolf, D. Dornisch, and H. Schulz, Surf. Sci. **279**, 199 (1992).
[60] A. D. Johnson, C. Norris, J. W. M. Frenken, H. S. Derbyshire, J. E. MacDonald, R. G. Van Silfhout, and J. F. van Der Veen, Phys. Rev. B **44**, 1134 (1991).
[61] D. Cvetko, L. Floreano, A. Crottini, A. Morgante, and F. Tommasini, Surf. Sci. **447**, L147 (2000).
[62] G. Le Lay, J. Kanski, P. O. Nilsson, U. O. Karlsson, and K. Hricovini, Phys. Rev. B **45**, 6692 (1992).
[63] A. D. Laine, M. Deseta, C. Cepek, S. Vandré, A. Goldoni, N. Franco, J. Avila, M. C. Asensio, and M. Sancrotti, Phys. Rev. B **57**, 14 654 (1998).
[64] A. D. Laine, M. Deseta, C. Cepek, S. Vandré, A. Goldoni, N. Franco, J. Avila, M. C. Asensio, and M. Sancrotti, Surf. Sci. **402–404**, 871 (1998).
[65] D. Cvetko, L. Floreano, A. Crottini, A. Morgante, and F. Tommasini, Surf. Sci. **447**, L147 (2000).
[66] X. J. Chen, A. C. Levi, and E. Tosatti, Nuovo Cimento D **13**, 919 (1991).
[67] A. Santoni, L. Petaccia, V. R. Dhanak, and S. Modesti, Surf. Sci. **444**, 156 (2000).
[68] A. D. Laine, M. Deseta, C. Cepek, S. Vandré, A. Goldoni, N. Franco, J. Avila, M. C. Asensio, and M. Sancrotti, Surf. Sci. **402–404**, 875 (1998).
[69] H. Noro and T. Ichikawa, Jpn. J. Appl. Phys., Part 1 **24**, 1288 (1985).
[70] T. Ichikawa, T. Sueyosi, T. Sato, M. Iwatsuki, F. Udagawa, and I. Sumita, Solid State Commun. **93**, 541 (1995).
[71] Y. Yamamoto, S. Ino, and T. Ichikawa, Jpn. J. Appl. Phys., Part 1 **25**, L331 (1986).